Qualitative Theory of Dynamical Systems (2025) 24:66
https://doi.org/10.1007/s12346-025-01227-9

Phase Portraits of the Family IV of the Quadratic Polynomial Differential Systems

Joan Carles Artés[1] · **Laurent Cairó**[2] · **Jaume Llibre**[1]

Received: 27 August 2024 / Accepted: 15 January 2025 / Published online: 5 February 2025

Abstract
In the $\mathbb{R}^2$ plane, the simplest non-linear differential systems are the quadratic polynomial differential systems. This type of differential systems have been studied intensively because of its non-linearity and wide range of applications. These systems have been classified into ten classes. In this article, we characterize in the Poincarè disk all topologically different phase portraits for one of these classes. Concretely we provide the complete study of the geometry of family IV. The family IV is six-dimensional and is reduced to several subfamilies which are three-dimensional. We give the bifurcation diagram of each specific normal form using invariant polynomials. The split of all quadratic systems in ten subfamilies could have been a good way to find all possible phase portraits of quadratic systems, if all ten families could have been studied completely. All families are six-dimensional and some of them can even be divided in several subfamilies with fewer parameters. However, certain families (I, II, and III) are too generic and cannot be reduced enough to allow its complete study. Regardless, this division of quadratic systems has been useful to study several families of quadratic systems having some other properties, and it is worth trying to get as many of them as possible studied in a complete way.

Keywords Quadratic vector field · Quadratic system · Phase portrait

Mathematics Subject Classification Primary 34C05 · 34A34 · 34C14

✉ Joan Carles Artés
joancarles.artes@uab.cat

Laurent Cairó
lcairo85@orange.fr

Jaume Llibre
jaume.llibre@uab.cat

[1] Departament de Matemàtiques, Universitat Autònoma de Barcelona, 08193 Bellaterra, Barcelona, Catalonia, Spain

[2] Institut Denis Poisson, Université d'Orleans, Collegium Sciences et Techniques, Batiment de Mathématiques, Rue de Chartres BP6759, 45067 Orléans, Cedex 2, France

1 Introduction and Statement of the Main Results

A *quadratic polynomial differential system* usually simply called *quadratic system* is a planar differential system of the form

$$\dot{x} = P(x, y), \qquad \dot{y} = Q(x, y), \tag{1}$$

where P and Q are real polynomials in the variables x and y whose maximum degree is two. As usual, the dot indicates the derivative with respect to the time t.

The interest in the study of quadratic systems began in the early 20th century. Coppel in [17] mentions that the first work on quadratic systems was published by Büchel [13] in 1904. Two studies on quadratic systems were published in 1966 by Coppel [17], and in 1982 by Chicone and Tian [16].

Quadratic systems have been studied intensively in recent decades and many interesting results have been published, see for example the books [12, 20, 29] and the references cited therein. But we are still far from a complete understanding of the dynamics of these systems.

In the paper [19] it was proved that an arbitrary quadratic system, after an affine change of variables and a change of scale of the time variable if necessary, becomes a quadratic system of the form

$$\dot{x} = P(x, y), \qquad \dot{y} = Q(x, y) = d + ax + by + \ell x^2 + mxy + ny^2, \tag{2}$$

where the differential equation $\dot{x} = P(x, y)$ is one of the following ten:

$$\begin{array}{ll} \text{(I)} \quad \dot{x} = 1 + xy, & \text{(VI)} \quad \dot{x} = 1 + x^2, \\ \text{(II)} \quad \dot{x} = xy, & \text{(VII)} \quad \dot{x} = x^2, \\ \text{(III)} \quad \dot{x} = y + x^2, & \text{(VIII)} \quad \dot{x} = x, \\ \text{(IV)} \quad \dot{x} = y, & \text{(IX)} \quad \dot{x} = 1, \\ \text{(V)} \quad \dot{x} = -1 + x^2, & \text{(X)} \quad \dot{x} = 0. \end{array}$$

Among these ten families, some have already been studied as for example VII and VIII in [15]. Some (IX and X) are so trivial to study that they do not even deserve to become an article. Family VI implies the existence of two parallel complex straight lines and all the phase portraits have already been obtained in [5]. The V family implies the existence of two real parallel lines and is not yet complete, but all the configurations and singularities have already been found in [14]. So it's a good candidate for further study. On the other hand, we discovered some schortcomings in [15]. So the families VII and VIII will be studied again in a future article using the techniques used here. The three families (I, II and III) are too generic and cannot be fully studied using the tools of this paper (they require a study with 4 or 5 parameters). Finally the Family IV studied here represents a strong important challenge that can be met with our technique.

A polynomial differential system in $\mathbb{R}^2$ can be analytically extended to the Poincarè disk, and in this way we can study the orbits of the polynomial differential system in a neighborhood of infinity. For more details, see [18, Chapter 5]. Roughly speaking,

the Poincarè disk is the closed unit disk centered at the origin of $\mathbb{R}^2$ whose interior has been identified with $\mathbb{R}^2$ and its boundary, the circle $\mathbb{S}^1$, is identified with the infinity of $\mathbb{R}^2$.

The objective of this paper is to classify the topologically distinct phase portraits in the Poincaré disk of the family of quadratic systems IV, i.e. of the systems

$$\dot{x} = y, \qquad \dot{y} = d + ax + by + \ell x^2 + mxy + ny^2. \tag{3}$$

Our main result is the following:

Theorem 1.1 *The family of quadratic systems* IV *has at least* 85 *topologically distinct phase portraits in the Poincarè disk given in* Figs. 1, 2, 3 and 4.

Remark 1.2 Family IV has been divided into four subfamilies A, B, C and D. Phase portraits are labeled according to the subfamily and to the parts of the bifurcation diagram where they appear. So we could therefor have a phase portrait named $A1S_2$ appeared in system A, and another phase portrait named $C1S_2$ in system C which they are different. Its labels can be different for two topologically equivalent phase portraits occurring in distinct subsets. In Table 1 (in Sect. 4) we have extracted a representative from each set of topologically equivalent phase portraits, labeled according to the subset in which they appear. For the subsets for which we have obtained a topologically equivalent phase portrait, see Appendix A, where we place all topologically equivalent phase portraits in the same horizontal block. Since most of the phase portraits that appear in systems B, C and D, have previously appeared in system A, they receive the definitive name from A. In the study of the different systems, we will not add the letters A, B, C or D to the bifurcation diagrams so not to avoid overloading the image, the subfamily will appear simply in the caption.

The separatrices have been drawn in widebroad black and some orbits needed to complete the phase portrait have been added in fine black.

This paper is organized as follows: In Sect. 2, we recall the basic tools we need for proving Theorem 1.1. In Sect. 3 we apply these tools to our quadratic system in order to obtain the phase portraits. In Sect. 4 we give the tool to extract the representative from each set of topologically equivalent phase portraits, thus proving Theorem 1.1 and we also give a table to relate all the topologically equivalent phase portraits with their representatives. We add an Appendix in which we compare the results of this paper with a recently published paper [2] which is entirely covered by the present paper.

2 Preliminary Definitions

Usually the study of the phase portrait of a polynomial differential system begins with the analysis of the local phase portraits of its equilibria, finite and infinite in the Poincarè disk. We then study its separatrix connections and limit cycles.

However this technique requires us to start from a relatively simple normal form in which at least finite singularities are easy to determine, so that the Jacobian matrices

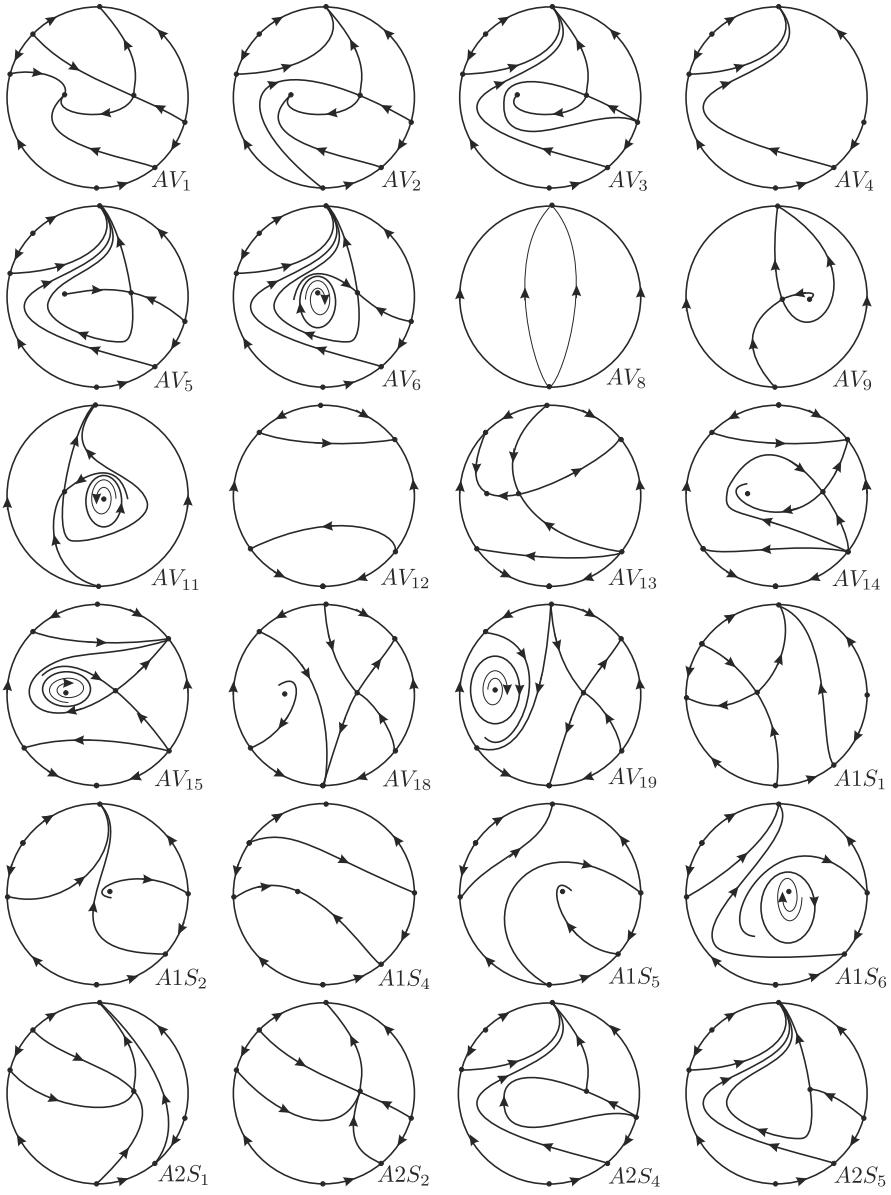

Fig. 1 The global phase portraits of systems (3)

of all singularities can be computed. Moreover, the classical technique is difficult to use when the number of parameters is greater than 2. Recently, a new technique for studying bifurcation diagrams of quadratic systems has been introduced and used in several papers (see [3, 4, 6–10]). The new technique concerns the theory of invariants applied to polynomial differential systems and is fully described in the book [12]. As

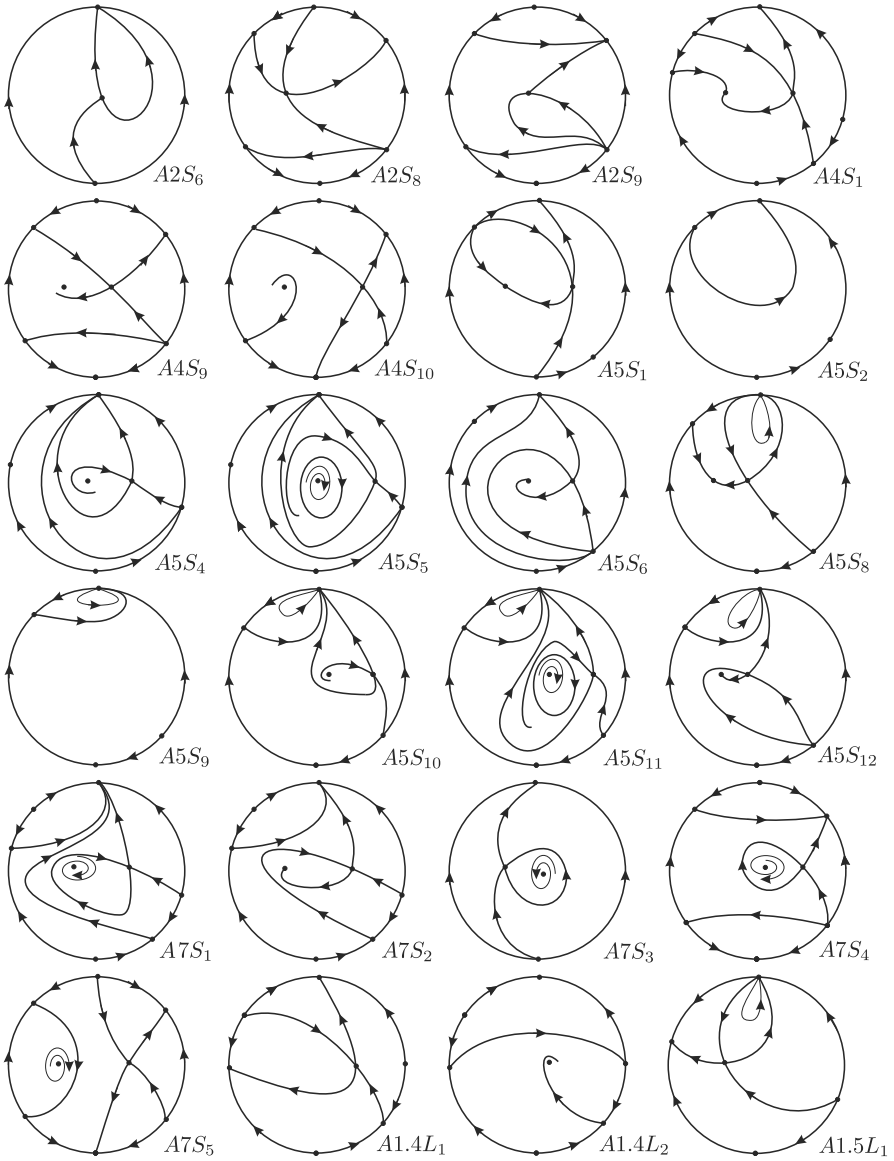

Fig. 2 The global phase portraits of systems (3) (cont.)

we are dealing with a six-parameter system (which we can later reduce to three), we will use the new technique.

In the following subsection we recall the basic notations and definitions we will use to study the local phase portraits of finite and infinite equilibrium points.

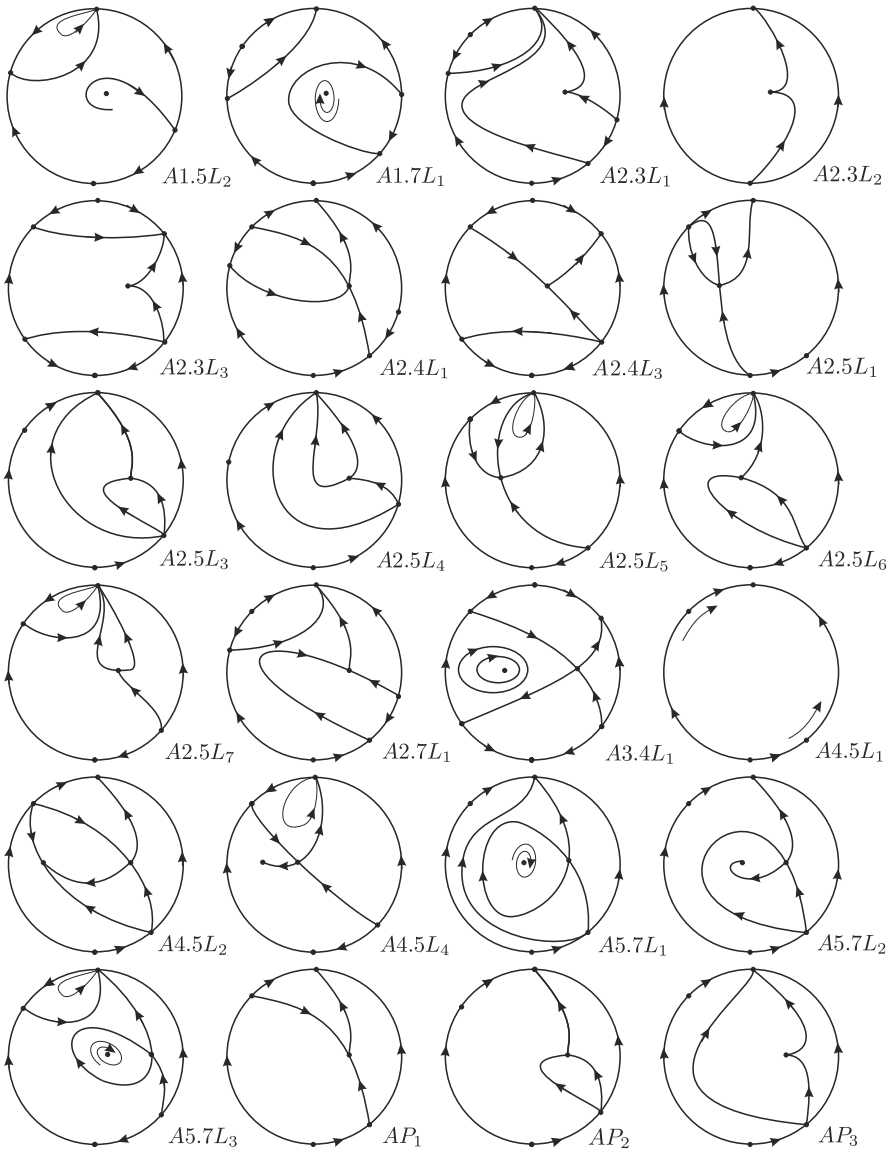

Fig. 3 The global phase portraits of systems (3) (cont.)

2.1 Equilibrium Points

The point $q \in \mathbb{R}^2$ is an *equilibrium point* of the polynomial differential system (1) when $P(q) = Q(q) = 0$.

The equilibrium point q is *hyperbolic* if the real part of the two eigenvalues of the Jacobian matrix of system (1) at q is non-zero. Local phase portraits of hyperbolic equilibrium points are well known, see for example [18, Theorem 2.15].

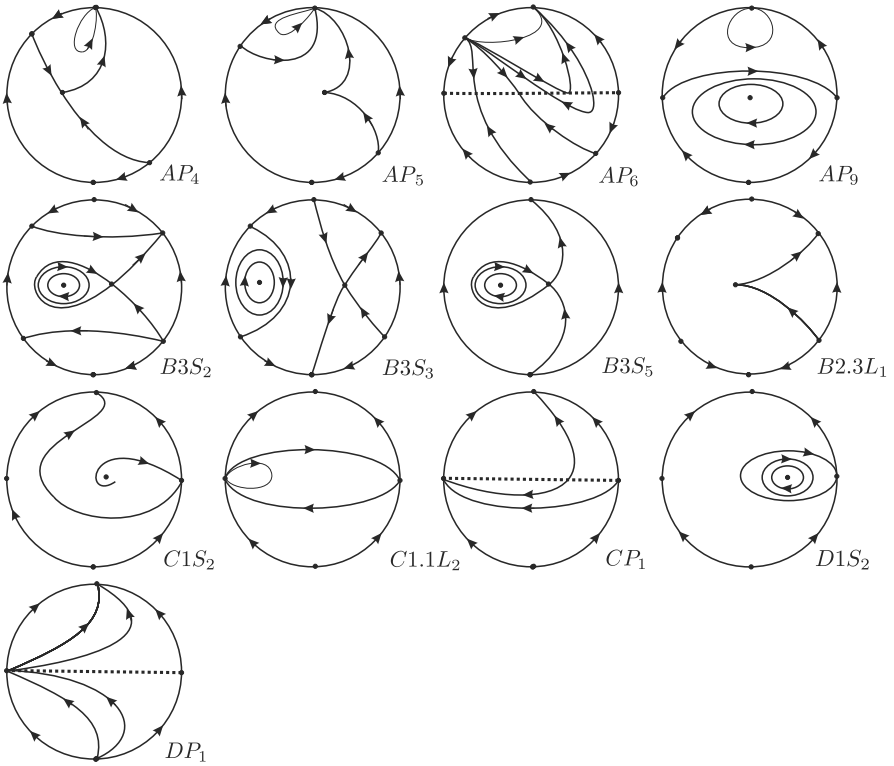

Fig. 4 The global phase portraits of systems (3) (cont.)

The equilibrium point q is *elemental* if neither of the two eigenvalues of the Jacobian matrix of system (1) at q is zero. This definition includes all hyperbolic singularities as well as the rest of the singularities of multiplicity one, i.e. weak foci and centers.

The equilibrium point q is *semi-hyperbolic* or *semi-elemental* if one of the eigenvalues of the Jacobian matrix of system (1) at q is zero and the other non-zero. The local phase portraits of semi-hyperbolic equilibrium points are well known, see for instance [18, Theorem 2.19].

The equilibrium point q is *nilpotent* if both eigenvalues of the Jacobian matrix of system (1) at q are zero, but this matrix is not the zero matrix. Local phase portraits of nilpotent equilibrium points are well known, see for instance [18, Theorem 3.5].

The equilibrium point q is *intricate* or *linearly zero* if the Jacobian matrix of system (1) at q is the zero matrix. The local phase portraits of a degenerate equilibrium point must be studied using special variable changes called blow-ups, see for instance [1].

2.2 Reducing the Number of Parameters of System (3)

Since we are starting with a family of 6 parameters, we will reduce system (3) to a set of several subfamilies of systems with fewer parameters.

First we assume $m \neq 0$ in system (3). Then by the rescaling[1] $(x, y) = (\bar{x}/m, \bar{y}/m)$ we can assume $m = 1$ and by a change of the variables $(x, y) = (\bar{x} - b, \bar{y})$, we can have a new subfamily of systems (4) without the y term, i.e. a system with $b = 0$:

$$\dot{x} = y, \qquad \dot{y} = d + ax + \ell x^2 + xy + ny^2, \tag{4}$$

which has just four parameters. Again, we will distinguish between $\ell \neq 0$ and $\ell = 0$. In the first case a change of time like $(x, y, t) = (\ell\bar{x}, \ell^2\bar{y}, \bar{t}/\ell)$ allows to assume $\ell = 1$ and obtain the 3-parameters systems (5).

$$\dot{x} = y, \qquad \dot{y} = d + ax + x^2 + xy + ny^2. \tag{5}$$

If $\ell = 0$, we can distinguish the case $n \neq 0$ from the case where $n = 0$. In the first case, we can rescaling $(x, y) = (\bar{x}/n, \bar{y}/n)$ and assume $n = 1$, obtaining the system:

$$\dot{x} = y, \qquad \dot{y} = d + ax + xy + y^2, \tag{6}$$

and when $n = 0$ we obtain the system

$$\dot{x} = y, \qquad \dot{y} = d + ax + xy. \tag{7}$$

These last two subfamilies of systems have only two parameters (a, d). The set of systems (5), (6) and (7) will be called the set A, which includes all cases with $m = 1$.

Assume now $m = 0$ in system (3) and $\ell \neq 0$, then by the rescalling $(x, y) = (\bar{x}/\ell, \bar{y}/\ell)$ we can assume $\ell = 1$, and by a change of the variables $x = \bar{x} - a/2$ we can cancel the coefficient of x in the second equation, i.e. with $a = 0$ obtaining systems (8):

$$\dot{x} = y, \qquad \dot{y} = d + by + x^2 + ny^2, \tag{8}$$

i.e. systems with three parameters, which we denote by the set B.

Assume now $m = \ell = 0$ in systems (3). Then we may assume $n \neq 0$ (otherwise the systems would be lineal). Then by the rescalling $(x, y) = (\bar{x}/n, \bar{y}/n)$ we can assume $n = 1$. Now we may also consider the cases $b \neq 0$ and $b = 0$. If $b \neq 0$ a change like $(x, y, t) = (\bar{x}, b\bar{y}, \bar{t}/b)$ will maintain the coefficient 1 in y^2 of the second equation and will produce a coefficient 1 in y. So, if $b \neq 0$ we may assume $b = 1$ obtaining systems (9) with just two parameters (d, a):

$$\dot{x} = y, \qquad \dot{y} = d + ax + y + y^2, \tag{9}$$

We denoted these systems as set C.

[1] All the rescalings, changes of time and traslations we will do in this section, produce also some changes in the rest of parameters, but for simplicity, we rename the new formed parameters and variables with the original ones.

Table 1 Topological equivalences

Presented phase portrait	Multiple singularity	Weak focus	Weak saddle	Invariant straight line	Other reasons
AV_1					
			$A3S_{2,8}$	$A4S_{2-5}$	
				$A4.4L_1$	
AV_2					AV_7
			$A3S_{1,3}$		
AV_3					
			$A3S_4$		
AV_4					
	$A1.2L_{1-2}$				
AV_5					
		$A3S_5$			
AV_6					
AV_8	BV_5				
	$B5S_1$		$B3S_4$		
			$B3.5L_1$		
AV_9	BV_6				AV_{10}
	$B5S_2$	$A3S_6$	$A3S_7$		
AV_{11}					
AV_{12}	BV_1				
		$B3S_1$			
AV_{13}	BV_2				AV_{17}
		$A3S_9$		$A4S_{7,8}, B4S_3$	
AV_{14}	BV_3				AV_{16}
		$A3S_{10,11}$			
AV_{15}					
AV_{18}	BV_4				AV_{20}
		$A3S_{8.12}$			
AV_{19}					
$A1S_1$					$A1S_3$
		$A1.3L_{2,3}$		$A1.4L_4$	
$A1S_2$					
		$A1.3L_1$			
$A1S_4$					
				$A1.4L_3$	
$A1S_5$					
$A1S_6$					
$A2S_1$					$A2S_3$
$A2S_2$					

Table 1 continued

Presented phase portrait	Multiple singularity	Weak focus	Weak saddle	Invariant straight line	Other reasons
$A2S_4$					
$A2S_5$					
$A2S_6$	$B2S_3$				$A2S_7$
	$B2.5L_1$				
$A2S_8$	$B2S_1$				$A2S_{11}$
$A2S_9$	$B2S_2$				$A2S_{10}$
$A4S_1$					$A4S_6$
$A4S_9$	$B4S_1$				$A4S_{12}$
		$A3.4L_2$			
$A4S_{10}$	$B4S_2$				$A4S_{11}$
		$A3.4L_3$			
$A5S_1$					$A5S_7$
			$A3.5L_{6,7}$		
$A5S_2$					$A5S_3$
$A5S_4$					
		$A3.5L_4$			
$A5S_5$					
$A5S_6$					
			$A3.5L_5$		
$A5S_8$					
			$A3.5L_3$	$A4.5L_3$	
$A5S_9$					AP_7
$A5S_{10}$					
		$A3.5L_1$			
$A5S_{11}$					
$A5S_{12}$					
			$A3.5L_2$		
$A7S_1$					
$A7S_2$					
$A7S_3$					
$A7S_4$					
$A7S_5$					
$A1.4L_1$					
			AP_{13}		
$A1.4L_2$					
$A1.5L_1$	$C1S_1, D1S_1$				
					AP_8

Table 1 continued

Presented phase portrait	Multiple singularity	Weak focus	Weak saddle	Invariant straight line	Other reasons
$A1.5L_2$					
$A1.7L_1$					
$A2.3L_1$					
$A2.3L_2$	$B2.3L_1$				
	BP_1				
$A2.3L_3$					
$A2.4L_1$	$A2.4L_2$				
$A2.4L_3$	$A2.4L_4$				
	$B2.4L_1$				
$A2.5L_1$	$A2.5L_2$				
$A2.5L_3$					
$A2.5L_4$					
$A2.5L_5$					
$A2.5L_6$					
$A2.5L_7$					
$A2.7L_1$					
$A3.4L_1$	$B3.4L_1$				
$A4.5L_1$	$C1.1L_1$				
	$D1.1L_1$				
$A4.5L_2$					
			AP_{12}		
$A4.5L_4$					
			AP_{10}		
$A5.7L_1$					
$A5.7L_2$					
			AP_{11}		
$A5.7L_3$					
AP_1					
AP_2					
AP_3					
AP_4					
AP_5					
AP_6					
AP_9					
$B3S_2$					
$B3S_3$					
$B3S_5$	$B3.5L_2$				
$B2.3L_1$					

Table 1 continued

Presented phase portrait	Multiple singularity	Weak focus	Weak saddle	Invariant straight line	Other reasons
$C1S_2$					
$C1.1L_2$	$D1.1L_2$				
CP_1					
$D1S_2$					
DP_1					

Finally, assume $m = \ell = b = 0$ in systems (3) and again $n = 1$ for the same reason as above, so the systems are reduced to one subfamily with only two parameters:

$$\dot{x} = y, \qquad \dot{y} = d + ax + y^2, \tag{10}$$

We denoted these systems as set D. We could even split these systems in some families with only one parameter plus some concrete systems, but these systems are simple enough and further reductions complicate the study instead of simplifying it.

2.3 Invariants

In order to obtain the bifurcation diagram of the different families of systems, we use the concept of algebraic invariant and comitant as formulated by the Sibirsky School for differential equations. For a summary of the general theory of these polynomial invariants and their relevance to work with polynomial differential systems, see [12, Chapter 5]. We begin this section by presenting the value of algebraic invariants and comitants (with respect to the normal form (3)) that are relevant to our study.

In what follows we will talk about bifurcation surfaces, but such surfaces sometimes will be hypersurfaces, or surfaces, or lines or points.

2.3.1 Algebraic Bifurcation Surfaces

The book [12] contains the formulas that give the bifurcation hypersurfaces of singularities in $\mathbb{R}^{12}$, produced by changes that may occur in the local nature of some or all singular points, finite or infinite. These bifurcation hypersurfaces are all algebraic.

($\mathcal{S}_1$) The invariants/comitants μ_i (from $i = 0, \ldots, 4$) determine how many finite singular points have escaped to infinity. For the general family of systems IV we have that $\mu_0 = \mu_1 = 0$, i.e. always two finite singularities have already escaped to infinity. Then we have that $\mu_2 = \ell(\ell x^2 + mxy + ny^2)$, $\mu_3|_{\ell=0} = -ay(mxy + ny^2)$ and $\mu_4|_{\ell=a=0} = dy^2(mxy + ny^2)$. In other words, discarding the case $\ell = m = n = 0$ which is linear, we have: a) if $\ell \neq 0$ no other finite singularity have escaped to infinity; b) if $\ell = 0 \neq a$ exactly three finite singularities have escaped to infinity; c) if $\ell = a = 0 \neq d$ all four finite singularities have escaped to infinity. The case $\ell = a = d = 0$ causes all $\mu's$ disappear, implying that there is an infinite number of

finite singularities. So, for the sets of systems B, we will not use invariant μ_2 because it will always be non-zero. For systems A, this surface will coincide with one slice ruled by systems (6). And for the set of systems C and D, we will have $\mu_2 = 0$ and therefore all the cases of systems C and D belong to $(\mathcal{S}_1)$. In both systems, the case $a = d = 0$ will produce *degenerate systems* (a system where there is a common factor between the defining functions).

$(\mathcal{S}_2)$ This is the bifurcation surface due to multiplicity of finite singularities, which contains the values for which at least two finite singular points coalesce. Since our general system already has two finite singularities coalesced with infinite singularities, we do not need to worry about higher degeneracies. This phenomenon is detected by the invariant $\mathbb{D}$ which for family IV is $\mathbb{D} = 48\ell^2(a^2 - 4d\ell)(4\ell n - m^2)$. There is one particular case in which both finite singularities will coalesce with the other two "finite" singularities which are already at infinity. This fact will be captured by the invariant $\mathbb{U}$ and will be applied in the proper places of the text.

$(\mathcal{S}_3)$ This bifurcation surface will contain the points on the parameter space for which there is a weak singularity, which may be a weak focus or a weak saddle. This is governed by the invariant $\mathcal{T}_4$ which for the whole family IV of systems is $\mathcal{T}_4 = n(4\ell n - m^2)(-abm + b^2\ell + dm^2)$. So this surface $(\mathcal{S}_3)$: $n(4\ell n - m^2)(-abm + b^2\ell + dm^2) = 0$ will appear in many bifurcation diagrams.

$(\mathcal{S}_5)$ This is the bifurcation surface due to the multiplicity of infinite singularities, which contains the values for which at least two infinite singular points coalesce. This phenomenon is detected by the invariant polynomial η (see [12, Lemma 5.5]) which, for the family of systems IV, is $\eta = n^2(m^2 - 4\ell n)$.

If $\eta = 0$ then the next comitants to consider are $\tilde{M} = -8(-3\ell n x^2 + m^2x^2 + mnxy + n^2y^2)$ and $C_2 = -x(\ell x^2 + mxy + ny^2)$ for family IV. Since $C_2 \not\equiv 0$ for non-linear systems, we have that if $\eta = \tilde{M} = 0$ there will be an infinite triple singularity by coalescence of the three infinite singularities.

$(\mathcal{S}_4)$ This surface will contain the points of the parameter space where invariant straight lines can appear. These lines may or may not contain separatrix connections of different singularities. In some cases, this may involve a topological bifurcation (the invariant line is a separatrix connection) and, in others, a simple C^∞ bifurcation (the invariant line is not a separatrix connection). This bifurcation does not deal directly with singularities, and even the invariants governing it are given in [12, Page 130], their geometric meaning is not used there. It is widely used in Schlomiuk and Vulpe's papers [22–27] which deal with quadratic systems with invariant straight lines. Specifically, it is explained that there are three comitants: B_1, B_2 and B_3, and that $B_1 = 0$ is a necessary (but not sufficient) condition for a quadratic system to have an invariant straight line. If $B_1 = 0$ then $B_2 = 0$ is a necessary and sufficient condition for having invariant lines in two different directions (but it is possible for a line to be coalesced with infinity). This is the case in our family IV where $B_1 = 0$ and

$$\begin{aligned} B_2 = -648x^4(&a^4n^4 - 2a^3bmn^3 - a^3m^2n^2 + 2a^2b^2\ell n^3 + a^2b^2m^2n^2 + 2a^2b\ell mn^2 \\ &+a^2bm^3n - 8a^2d\ell n^4 + 2a^2dm^2n^3 - 2a^2\ell^2n^2 + 2a^2\ell m^2n - 2ab^3\ell mn^2 \\ &-3ab^2\ell m^2n + 8abd\ell mn^3 - 2abdm^3n^2 - 2ab\ell^2mn - ab\ell m^3 + 4ad\ell m^2n^2 \\ &-adm^4n - a\ell^2m^2 + b^4\ell^2n^2 + 2b^3\ell^2mn - 8b^2d\ell^2n^3 + 2b^2d\ell m^2n^2 + 2b^2\ell^3n \end{aligned}$$

$$+b^2\ell^2m^2 - 8bd\ell^2mn^2 + 2bd\ell m^3n + 2b\ell^3m + 16d^2\ell^2n^4 - 8d^2\ell m^2n^3$$
$$+d^2m^4n^2 + 8d\ell^3n^2 - 6d\ell^2m^2n + d\ell m^4 + \ell^4).$$

If $B_2 = 0$ we will have at least one invariant straight line. This formula will be conveniently reduced according to the different normal forms that we will be working with.

($\mathcal{S}_6$) This surface contains the points in parameter space where a finite node becomes focus. In other words, in a neighborhood of ($\mathcal{S}_6$), there exist a singular point that passes continuously from a node to a focus, or vice versa. This surface is a bifurcation surface from a geometrical point of view but not topological. Indeed, if we simply travers the surface ($\mathcal{S}_6$) in the bifurcation diagram, the topological phase portraits remain unchanged. However, this surface is relevant for locating regions where a limit cycle surrounding a finite antisaddlle cannot exist. In previous works using the same technique, this surface was included in the bifurcation diagram, thus increasing the number of parts into which the diagram divides the space of parameters. Moreover, this surface is rather complicated and we prefer to remove it from the bifurcation diagram, as it will never decide on its own whether topologically different phase portraits exist. In fact, we don't intend to use it again in the future, unless it is really relevant to a certain family. The invariant governing this phenomena is W_4 which for family IV is:

$$W_4 = n^2(4\ell n - m^2)^2(4a^3m^2 + a^2b^2m^2 - 8a^2b\ell m - 16a^2\ell^2 - 2ab^3\ell m$$
$$- 2abdm^3 - 16ad\ell m^2 + b^4\ell^2 + 2b^2d\ell m^2 + 32bd\ell^2m + d^2m^4 + 64d\ell^3).$$

2.3.2 Non-algebraic Bifurcation Surfaces

We will detect another bifurcation surface which is not necessarily algebraic. In such a non-algebraic surface, the family has a global connection of separatrices different from those given by ($\mathcal{S}_4$). The equation of this bifurcation surface can only be approximately determined using numerical tools. Using continuity arguments in phase portraits, we can prove the existence of this unnecessary algebraic component in the part where it appears, and we can verify it numerically. We will call this surface ($\mathcal{S}_7$).

2.3.3 Difference from Previous Works with Same Technique

The way in which the parameter space is studied in this article differs somewhat from that used in other similar papers (see [3, 4, 6–10]).

In these papers the authors started with one or more normal forms up to with five parameters and compacted the parameter space into the projective space $\mathbb{RP}^3$ (except in one case where they were able to work up to $\mathbb{RP}^4$). The point is that in all these previous works, all the parameters only affected the quadratic part of the system, allowing a time change that transformed points in $\mathbb{R}^4$ into equivalence classes in $\mathbb{RP}^3$. But this time we can't perform such a change, because we have parameters affecting all the coefficients of the second equation, which doesn't allow compactification in the projective space.

We will split the three-dimensional parameter space into two-dimensional slices in the same way as in the other papers, but this will correspond only to the affine part of the space. There will be no "slice" for the infinite part, as was the case in some previous works. In any case systems (6) can be considered as the "infinite slice" of the systems (5), and systems (6) and (7) can be considered as the equator of the compactified parameter space, but there will be no coincidence of phase portraits at opposite points of the equator, asis the case in projective space. There will be a certain symmetry, but not that.

The bifurcations which imply a topological change are drawn with a continuous line, and those which just imply a geometrical change with a dashed line.

In previous papers using the same technique, each part of the bifurcation parameter space received an exclusive code, even though it was obvious that its phase portrait would be topologically equivalent to that of a neighboring part. This led to a large number of parts. This time we decided to reduce this number and avoid giving names to parts separated by bifurcations that clearly imply no topological change in the phase portrait. So if one region has no label, take the same label of a region separated from it just by dashed lines.

In any case we will always find repeated phase portraits in some bifurcation diagrams within a subfamily, or between different subfamilies.

Regions of the bifurcation diagram that are three-dimensional have been labeled V_i where i is simply a cardinal. Two-dimensional regions of the bifurcation diagram were labeled kS_i where k represents the number of the bifurcation surface at which the region corresponds and i is a cardinal. Regions of the bifurcation diagram that are one-dimensional have been labeled $k.jL_i$ where k and j denote the two bifurcation surface numbers that intersect in this curve and i is a cardinal. If more than two surfaces intersect in the same curve, we've chosen the two with the greatest geometric significance. Regions of the bifurcation diagram that are zero-dimensional (just points) have been labeled as P_i where i is simply a cardinal.

3 Phase Portraits Search

3.1 Phase Portraits of Systems A

In our search for phase portraits of systems (4), we first assume systems with $\ell \neq 0$, i.e. systems (5). For these systems we divide the parameter space (a, d, n) into slices for n a fixed value and compute the bifurcations in each slice. For systems A the invariants are:

$$\begin{aligned} &\mathcal{T}_4 = dn(-1+4n),\ \mathbb{D} = 48(a^2-4d)(-1+4n),\ \eta = n^2(1-4\ell n)\\ &B_2 = -648x^4(1-a+d+2a^2n-6dn-adn-2a^2n^2-a^3n^2+8dn^2\\ &\qquad +4adn^2+d^2n^2+2a^2dn^3-8d^2n^3+a^4n^4-8a^2dn^4+16d^2n^4) \end{aligned} \quad (11)$$

From these slices, the slices $n_2 = n = 0$ and $n_4 = n = 1/4$ are singular, because they derive directly from the invariants $\mathbb{D}$, η and $\mathcal{T}_4$. When $n = 0$, then $B_2 = 648(-1+a-d)$ and when $n = 1/4$ then $B_2 = -(81/32)(-4+a)^4x^4$.

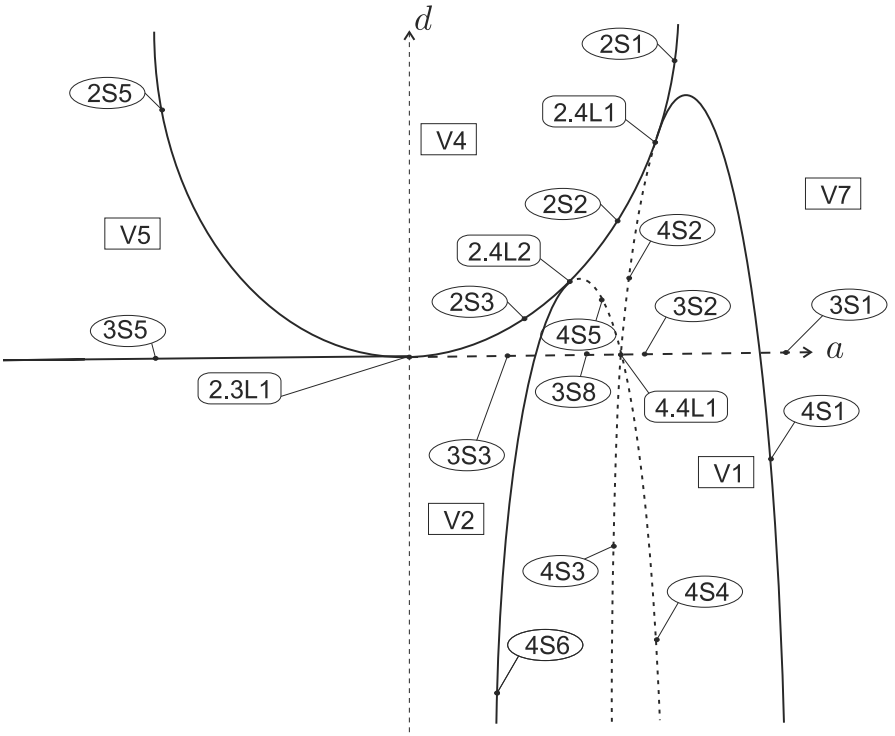

Fig. 5 Provisional bifurcation diagram for slice $n = n_3 = 1/8$

Except for the singular slices determined by the algebraic bifurcation surfaces there could be other singular slices which are given by triple intersections with one of the surfaces being $(\mathcal{S}_7)$. In almost all previous works using the same technique such non-algebraic singular slices exists and must be determined by numerical aproximations. However in this work, no such singular slice is needed to give a complete coherent bifurcation diagram.

We have two singular slices, so the bifurcation diagram at any slice $n \notin \{n_2, n_4\}$ will be topologically equivalent to any other slice in its same interval. In other words, we may choose one value $n_1 < n_2 = 0$, another $n_2 < n_3 < n_4$ and another $n_5 > n_4$ as generic slices. We take $n_1 = -1, n_3 = 1/8$ and $n_5 = 1$. Above all these slices (and below all them) we consider the system when $\ell = 0$ which is equivalent to consider as if all other parameters tend to $\pm\infty$. We call it $n = n_0 = -\infty$. As we have explained in Sect. 2.3.3, we cannot compactify our parameter space in a projective space, but we can still consider one of the slices as the "infinite" slice of another subset of the parameter space.

We start the study doing the complete bifurcation of slice $n_3 = 1/8$. We draw all the algebraic bifurcations obtained in Fig. 5.

The image we see in Fig. 5 does not need to be the exact reproduction of all the bifurcation curves. Many times the regions we obtain are very small and we do not have space enough to write the labels. So we show a topological equivalent diagram

with the original one, also respecting geometrical properties such as intersections and tangencies. For example surface $\mathcal{S}_4$ has two components when cutting this slice and both components are tangent to surface $\mathcal{S}_2$. We have labeled all the important regions according to the notation described above. We have already explained that we will not name every region when it is clear that such region will have the same topological phase portrait as a neighbor one. For example, we do not name the region delimited by $4S_3$ and $4S_4$ because the invariant straight lines obtained in these regions do not produce a separatrix connection and thus the phase portrait V_1 is not affected. In the same way we have not labeled the region above $3S_2$ and below $4S_1$ and $4S_2$, because the existence of a weak saddle at $3S_2$ does not affect V_1.

Now we must find with the help of the numerical program P4 [18] one phase portrait for each one of the regions, and we must check that such phase portrait is coherent in continuity with the phase portraits in the border of the region. But such coherence is not everywhere. For example the phase portrait that we obtain for region V_2 when we are close to $3S_5$ is not the same as the one we obtain when close to $4S_6$. And the reason is very simple, as we know in $3S_5$ there is a weak focus and close to it, either for $d > 0$ or $d < 0$ there must be a limit cycle. It happens to be for $d < 0$. Since such limit cycle does not exist near to $4S_6$, there must exist a separatrix connection (a loop) which delimits the region where the limit cycle exist. And this is the first part of surface $\mathcal{S}_7$ that we have detected by continuity and coherence arguments. We will denote such part of $\mathcal{S}_7$ as $7S_1$ (see Fig. 6) and the region with limit cycle as V_6 (we plot V_6 region in grey to indicate the existence of limit cycle). But this is not enough. The phase portrait that we obtain by perturbing the one in $7S_1$ is not still equivalent with V_2 close to $4S_6$. So we need a second separatrix connection which will take place on part $7S_2$ of $\mathcal{S}_7$ and it splits a new region V_3 from V_2.

We have already proved the existence of the regions $7S_1$ and $7S_2$ in some place of region V_2 of Fig. 5 but we have to prove where they start and end. Region V_6 must border $3S_5$ from the beginning to the end, because the limit cycle in V_6 comes from the weak focus in $3S_5$. The region $7S_1$ cannot cross $4S_6$ because the separatrix, which forms the loop, is also one of the separatrices which forms the straight line. If it crosses $3S_4$ then it should have to end at some point of surface $\mathcal{S}_2$ and the region with limit cycle would border a region with a saddle-node. But a saddle-node (of multiplicity 2) cannot produce limit cycles by perturbation. So the only remaining candidate is $2.3L1$ where we have a double point which is a cusp. And a cusp is compatible with the existence of a limit cycle in one of its perturbations. Since we have discarded all impossible limits for $7S_1$ and we have showed the compatibility of the only remaining one, this is the only possibility. On the other hand, $7S_1$ can only be extended to infinity. We do not know its asymptotic behavior but this is the only possibility.

We consider now the part $7S_2$. This part implies the existence of a separatrix connection between the finite saddle and an infinite saddle-node not forming an invariant straight line. So it cannot cross therfor $7S_1$ nor $4S_6$, because the finite separatrix is also needed there for other connections. So it must cross the surface $\mathcal{S}_3$ and end at some point of surface $\mathcal{S}_2$ between $2.3L_1$ and $2.4L_2$. It cannot enter into V_4 because there does not exist the finite saddle. Then taking points along $\mathcal{S}_2$ between $2.3L_1$ and $2.4L_2$ one can confirm numerically the existence of the phase portraits $2S_3$ and $2S_4$ implying then, the existence of the phase portrait $2.7L_1$.

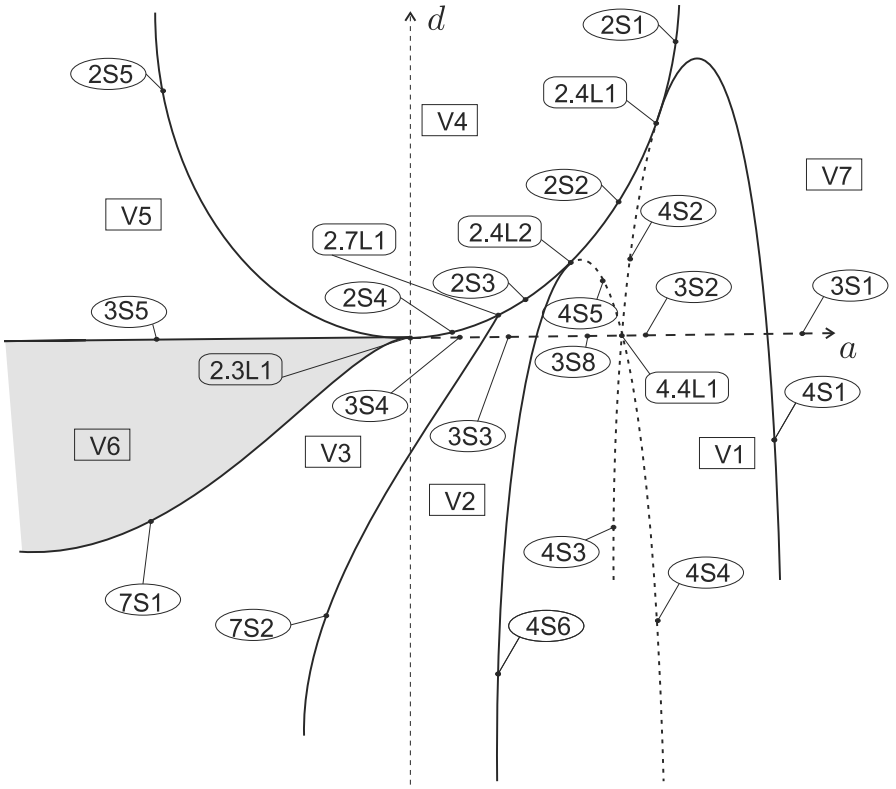

Fig. 6 Bifurcation diagram for slice $n = n_3 = 1/8$

Next we move to slice $n_4 = n = 1/4$. On this slice two geometrical facts occur. First this slice is in the surface $\mathcal{S}_5$ and this implies that always two infinite singularities coalesce (see Fig. 7). Thus every region in the slice $n = n_3 = 1/8$ will be bordered by a region in this slice. Most of the bifurcations that we see in the slice $n = n_3$ remain here, except that this surface $\mathcal{S}_4$ has a singularity in this slice and it corresponds with a single vertical straight line of multiplicity 4 ($B_2 = -81(a-4)^4x^4/32$).

The surface $\mathcal{S}_7$ extends along this slice while maintaining the same properties as explained above.

The next slice studied is the generic slice $n = n_5 = 1$. When we cross the slice $n = n_4$ we are also crossing bifurcation $\mathcal{S}_5$. For slices below $n = n_4$ we have that the invariant $\eta > 0$, thus we have three infinite singularities. But for slices above $n = n_5$ we have $\eta < 0$ and only one real infinite singularity. So the component $7S_2$ of the surface $\mathcal{S}_7$ which on the slice $n = n_4$ changed to $5.7L_2$ now cannot exist anymore. Moreover the surface $\mathcal{S}_4$ also disappears here from the real field after collapsing in parts $4.5L_1$, P_1 and $4.5L_2$. The rest of the regions remain equivalent to the previous slices, but all of them with a single infinite singularity (see Fig. 8).

We go back again to slice $n = n_3$ and consider now the next lower singular slice $n = n_2 = 0$. On this slice we still have $\eta = 0$, so two infinite singularities coalesce. And also

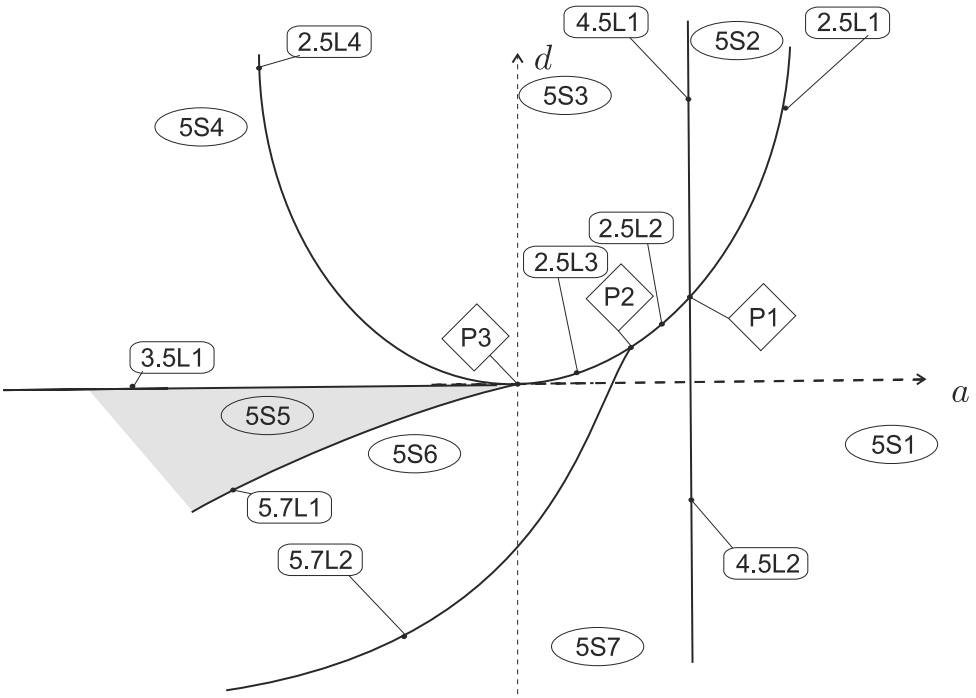

Fig. 7 Bifurcation diagram for slice $n = n_4 = 1/4$

the $\mathcal{S}_4$ bifurcation collapses in a single line of multiplicity 1 $B_2 = 648(a - 1 - d)x^4$. Again every region in the slice $n = n_3$ has a bottom cover in this slice. But now the component $7S_2$ of the surface $\mathcal{S}_7$ has disappeared because it collapses with part $4.5L_4$. Indeed, the infinite separatrix that produces the separatrix connection in $7S_2$ does not exist because we have the flat hyperbolic sector of a nilpotent elliptic saddle in its place. The phase portrait obtained in $4.5L_4$ is compatible by perturbations with V_1, V_2, V_3, $4S_6$ and $7S_2$ (see Fig. 9).

Now let's us move to the slice $n = n_1 = -1$. Note that since $\eta = n^2(m^2 - 4\ell cn)$, the sign of η did not change when going from $n > 0$ to $n < 0$. Thus we have again 3 infinite singularities. And quite many other changes happen too. On one side the surface $\mathcal{S}_4$ which on previous singular slices was only a straight line of multiplicity one because the remainder had escaped to infinity, now reappears from infinity forming again two pseudo-parabolas which continue having tangencies with surface $\mathcal{S}_2$ (see Fig. 10). As explained before, the shapes of the bifurcations that we draw are only topologically correct to allow the use of labels. Furthermore, when the surface $\mathcal{S}_4$ reappears from infinity along the surface $\mathcal{S}_3$ (see point $3.4L_1$) compresses the previous unbounded region V_6 (and its bottom cover $5S_{11}$) into a new bounded region V_{15}. And even more interesting, it brings from infinity a new region with limit cycle which is V_{19} which can easily be checked to be on the other side of surface $\mathcal{S}_3$.

Finally we study the slice $n = n_0 = -\infty$ (which can also be named $n = n_6 = \infty$ by means of a symmetry), or better said the systems (6) and (7) and we study them

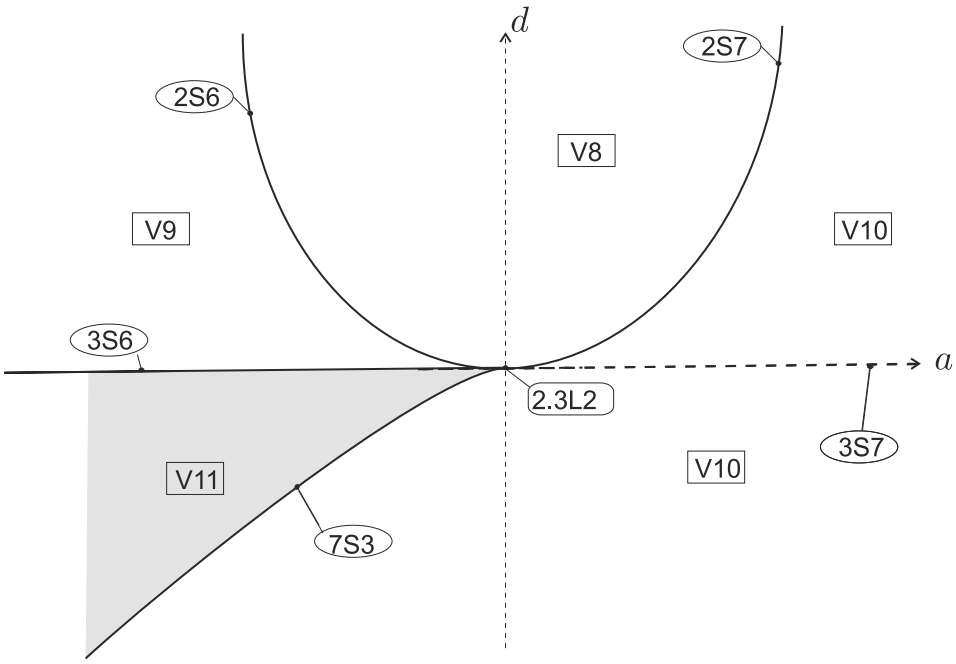

Fig. 8 Bifurcation diagram for slice $n = n_5 = 1$

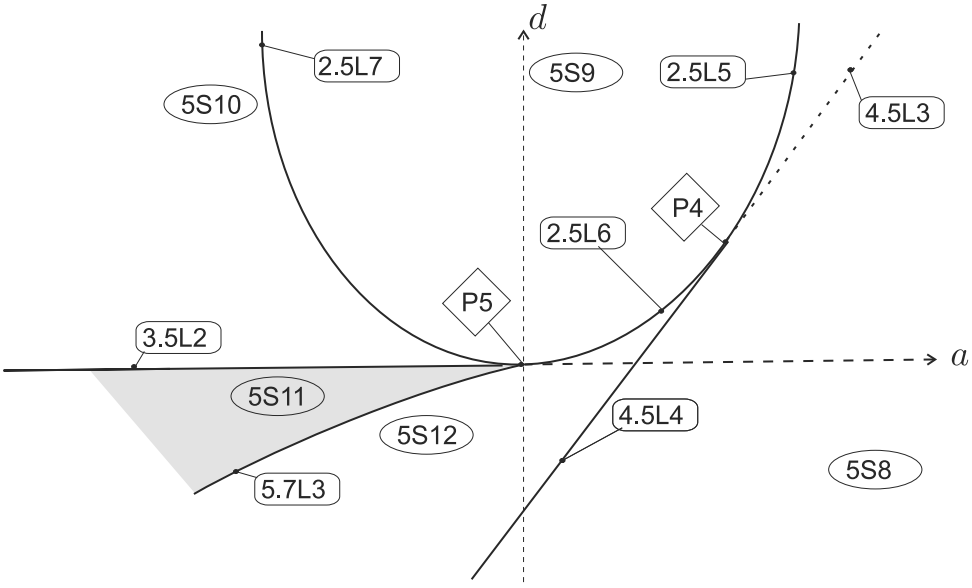

Fig. 9 Bifurcation diagram for slice $n = n_2 = 0$

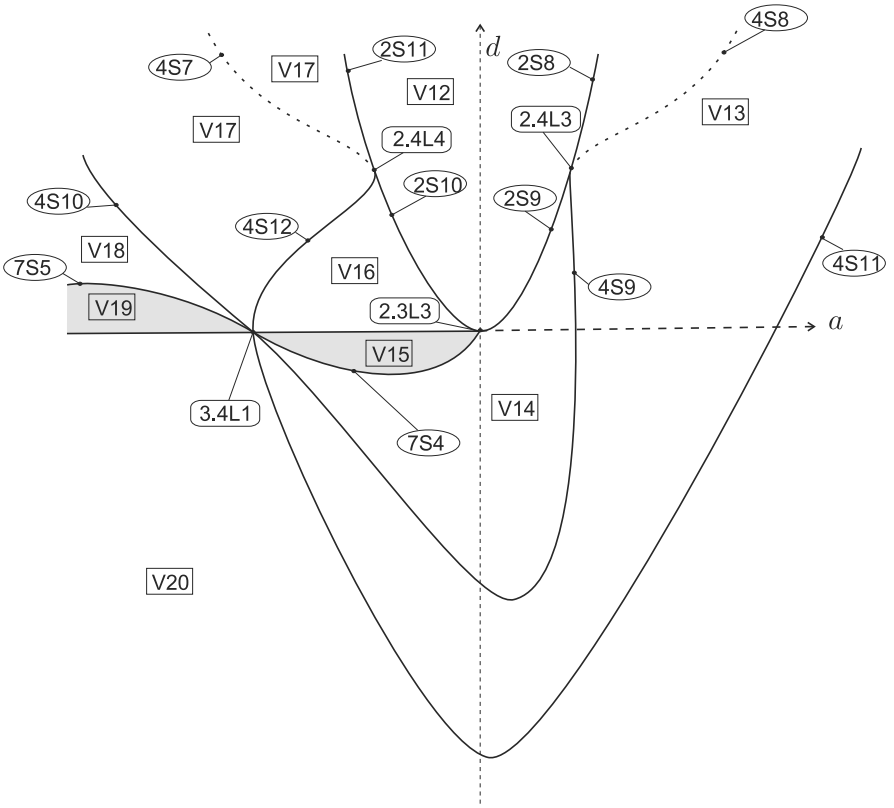

Fig. 10 Bifurcation diagram for slice $n = n_1 = -1$

both in a single compactified 2-dimensional parameter space. That is to say, we join both normal forms (6) and (7) in a single normal form with a parameter n in front of y^2 and consider a compactification of the parameter space by means of the change $(x, y, t) \to (x/n, y/n^2, nt)$) which allows us to work with the classes of equivalence $[d : a : n]$. Thus the normal form (6) corresponds to the affine part $[d : a : 1]$ and the normal form (7) corresponds to the infinite part $[d : a : 0]$. This is exactly the same that we have done when considering that normal form (6) corresponds to the "infinity" of normal form (5). We have drawn the outer circle of Fig. 11 in double color red and blue so to reflect that it belongs to both surfaces $\mathcal{S}_1$ and $\mathcal{S}_5$. We see here that the surface $\mathcal{S}_4$ becomes the union of two parabolas, because $B_2 = -648(a^2+d)(a^2-a-d)x^4$ (see Fig. 11). Moreover surface $\mathcal{S}_2$ collapses in a double straight line ($\mathbb{U} = a^2y^4(x+y)^2$), which means that both finite singularities have coalesced and simultaneously have escaped to infinity. If we see this slice as the topmost cover of the slice $n = n_5$ we see that the V_6 part has $1S_6$ as border, in which we have a similar phase portrait with limit cycle, but the saddle has escaped to infinity. And the part $7S_1$ cuts the slice $n = n_0$ into $1.7L_1$. Again we have to justify what happens with part $7S_2$. In this case we compare the phase portraits of $7S_2$ and $1.7L_1$ and we simply see that the finite saddle

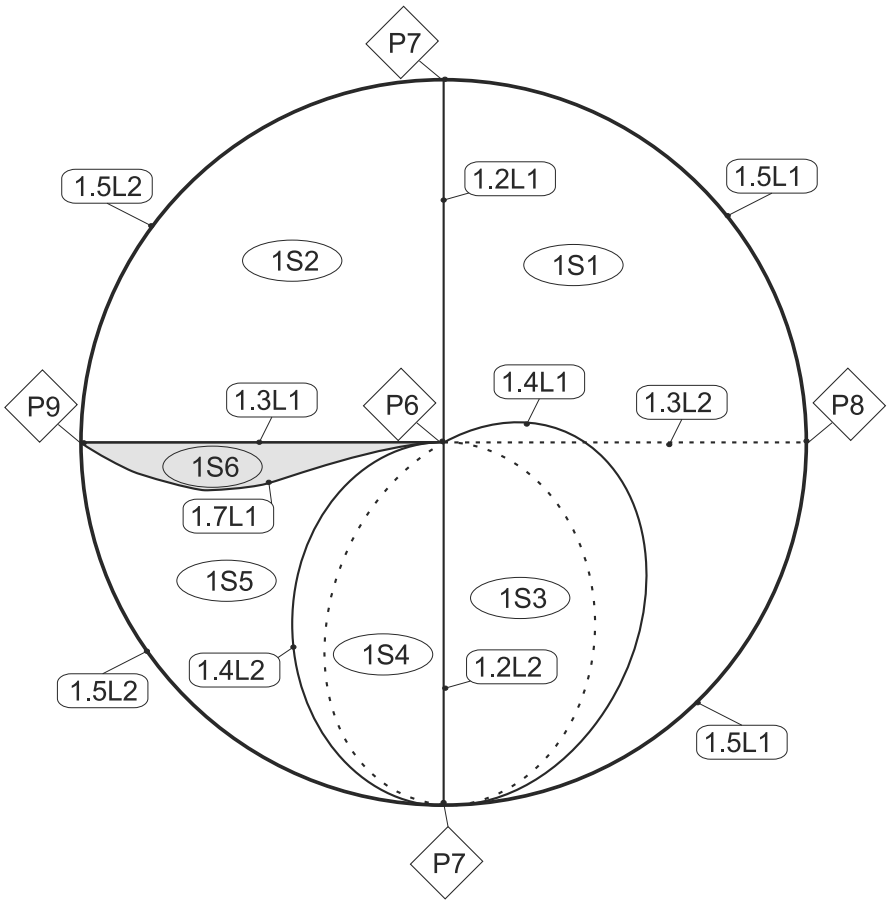

Fig. 11 Bifurcation diagram for slice $n = n_0 = \pm\infty$

has escaped to infinity while maintaining the separatrix connection. So $7S_2$ ends at $1.7L_1$. Since this slice may be considered either as the topmost slice, or the bottom most slice, similar arguments can be done to find the coherence between the parts of the slice $n = n_1$ with $n = n_0$.

Notice that all the slices we have taken could also be compactified into a disk form, and that all of them conform a set of ellipsoidal sectors which completely fill a 3-dimensional sphere, with the equator of the sphere being common to all slices.

In summary, we have covered all the detected regions in systems A, and moreover we have shown that there is no need of more slices above the topmost affine generic slice and below the bottom most generic one. As normally happens in this kind of studies, we cannot affirm that these are all the possible regions and phase portraits, but we can assure that the bifurcation diagram is coherent and complete in the sense that it does not need any other bifurcation to be explained.

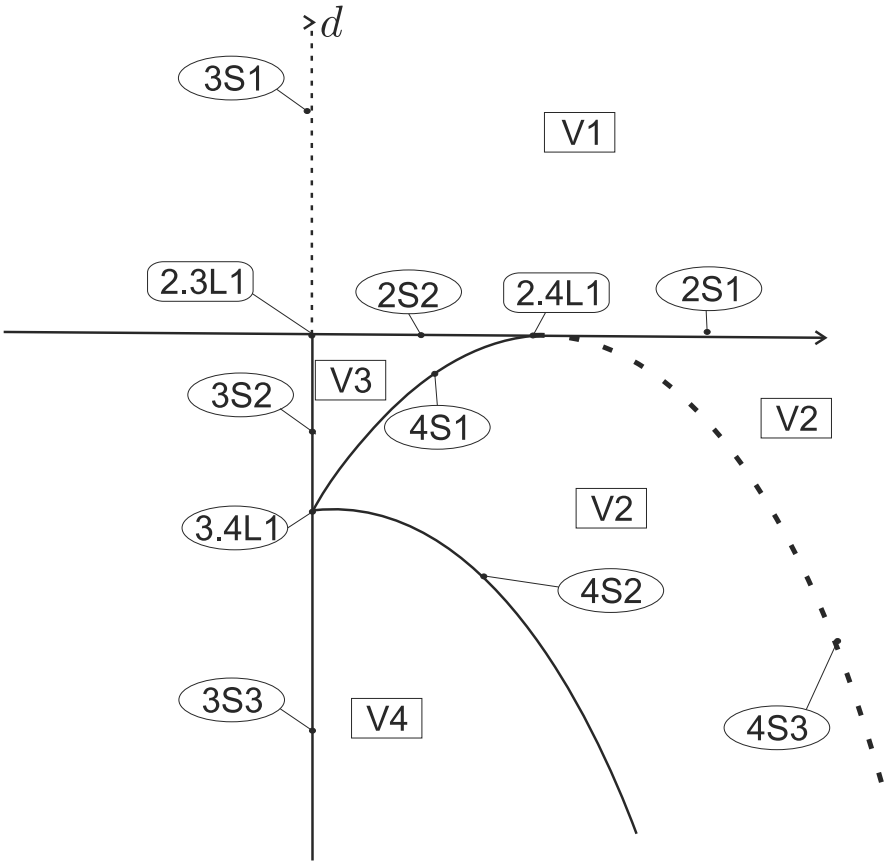

Fig. 12 (B) Bifurcation diagram for slice $n = n_1 = -1$

3.2 Phase Portraits of Systems B

We proceed in the same way as before for systems B. Now the 3-dimensional space of parameters is (b, d, n) and we slice it again along axis n. In this case it is easy to check that we need a unique singular slice $n_2 = 0$, and that we may take generic slices $n_1 = -1$ and $n_3 = 1$.

We start with the slice $n = n_1 = -1$. On this slice (in fact in all the bifurcation diagram for systems B) only surfaces $\mathcal{S}_2$, $\mathcal{S}_3$ and $\mathcal{S}_4$ are relevant. It is worth to notice that even we may have a weak focus in parts $3S_2$ and $3S_3$, there is no region with limit cycles. So there is a symmetry in the bifurcation diagram along the axis $b = 0$, and this is linked to the fact that the invariant $\mathcal{T}_4$ which rules surface $\mathcal{S}_3$ is a perfect square ($\mathcal{T}_4 = 4b^2\ell^2n^2$), so $\mathcal{T}_4$ cannot change sign, thus, the focus cannot change stability, thus either we have limit cycles on either side of $3S_3$ or not at all, which is what in fact happens (see Fig. 12).

Let us now consider the singular slice $n = n_2 = 0$. We must notice first that for this family $\eta = -4\ell n^3$ and $\tilde{M} = 8n(3\ell x^2 - ny^2)$. Thus, for $n = 0$ both vanish and

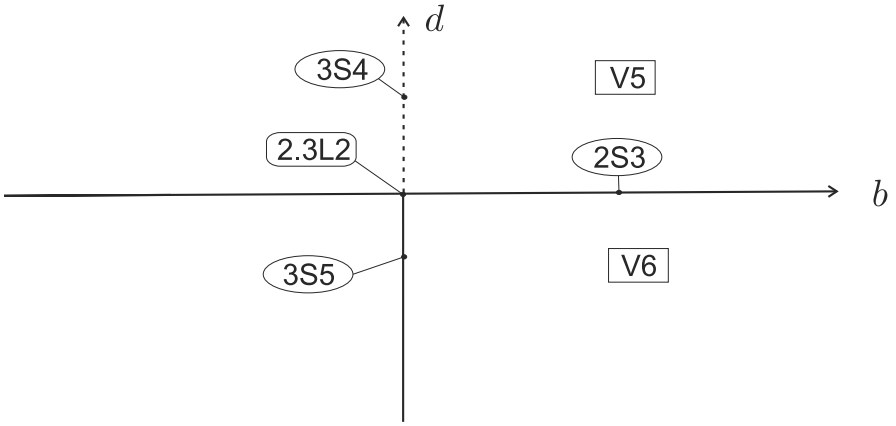

Fig. 13 (B) Bifurcation diagram for slice $n = n_2 = 0$

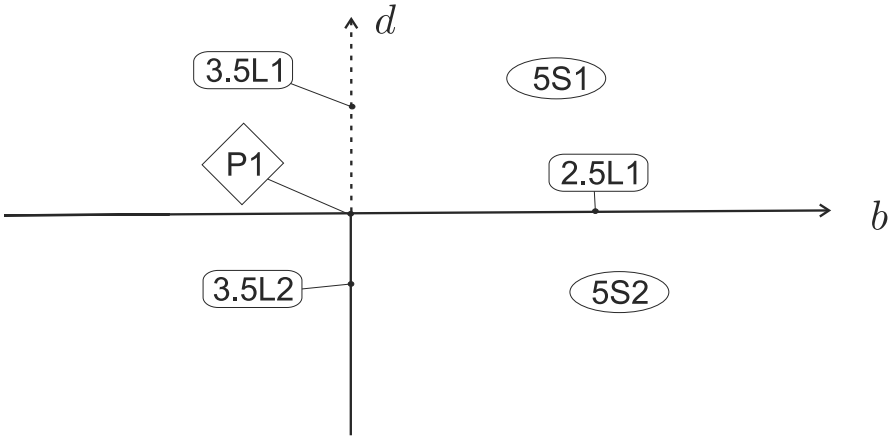

Fig. 14 (B) Bifurcation diagram for slice $n = n_3 = 1$

this means that all three infinite singularities have coalesced. Moreover $B_2|_{n=0,\ell=1} = -648x^4$ which means that surface $\mathcal{S}_4$ has escaped to infinity. So, the part $5S_2$ is the top cover of part V_3 (see Fig. 13).

The next slice is generic with $n = n_3 = 1$. The only relevant feature of this slice is that we do not see surface $\mathcal{S}_4$, and the reason is that the comitant B_2 is $-648x^4\left(b^4n^2 - 8b^2dn^3 + 2b^2n + 16d^2n^4 + 8dn^2 + 1\right)$ and solving this polynomial with respect of d we get the discriminant $-4nb^2$. So if $n > 0$ this surface does not have real representation (see Fig. 14).

When we studied the systems A we had a 4-parameter family that in order to be studied in a 3-dimensional way, we had to study it using differents charts in a compactified 3-parameter space. For systems B, we do not need such trick because we already have a simple 3-dimensional space.

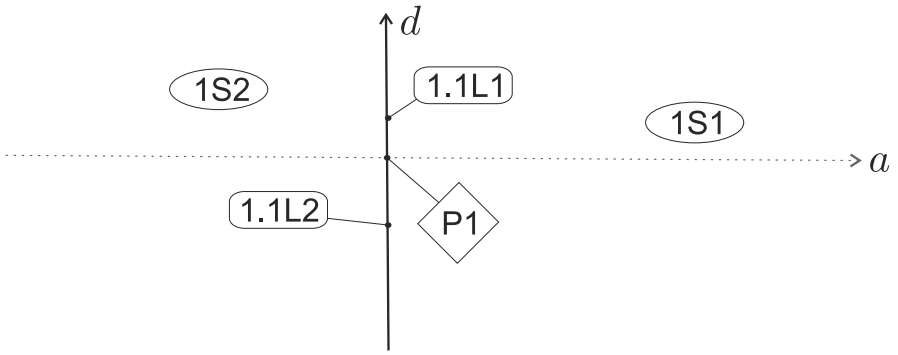

Fig. 15 Bifurcation diagram for systems C & D

3.3 Phase Portraits of Systems C and D

Systems C and D are only 2-parametric, and even they could be studied jointly in some compactifed parameter space, it is much simple to study them separately. In both systems we simply have a series of relevant comitants which are $\mu_2 = 0$, $\mu_3 = -ay^3$ and $\mu_4 = dy^4$. It is generically that one third singularity escapes to infinity. If $a = 0 \neq d$ the fourth point also escapes to infinity. But if $a = d = 0$ the system becomes degenerate. So the bifurcation diagram for both systems is exactly the same (see Fig. 15). But the regions of system C should be preceded with C and regions for system D should be preceded with D. Indeed we see that phase portraits for $C1S_1$, $C1.1L_1$ and $C1.1L_2$ are topologically equivalent to phase portraits for $D1S_1$, $D1.1L_1$ and $D1.1L_2$, but the phase portrait for $C1S_2$ is different from $D1S_2$, and the phase portrait for CP_1 is different from DP_1.

3.4 Possible Islands in the Parameter Space

In every paper of this kind, there is a compulsory subsection that we must add about this fact. We have done our bifurcation diagram for systems of family IV and our main theorem states that it exists 85 topologically different phase portrait in it. But this "it exists" schould not be read as "it exists exactly" but as "it exists at least". The reason is that there may be non algebraic bifurcations, mainly related to double limit cycles or separatrix connections which could escape to this study. In this family we cannot have double limit cycles since Rychov [21] already proved the uniqueness and hyperbolicity of the Class I.[2] But more separatrix connections could exist. However, since we have proved the completeness and coherence of the bifurcation diagram as it is given here, we have proved that no further bifurcation is needed in order to describe it. So, if any other separatrix connection were possible, this should have to take place at the border of a "bubble" (something topologically equivalent to a sphere of the proper

[2] The Class I must not be confused with the family I of (2), see the Appendix for more details.

dimension in the parameter space) and inside it, we could maybe have a different phase portrait. Since such bubbles, in case they exist, could have any small size, it is not worth trying to find them by a numerical search. It would already be worthless in a 2-dimensional space, even much more in a 3-dimensional one. This is why we have called them "islands". It is also worth to mention that in none of the previous families studied up to now with this technique, such an island has never been proved to exist.

4 Summing Up the Global Geometrical Properties of Quadratic Systems of Family IV: The Classification Theorem

In a bifurcation diagram we may have topologically equivalent phase portraits belonging to distinct regions of the parameter space. As here we have 174 distinct parts of the parameter space, to help us identify or to distinguish phase portraits, we need to introduce some topological invariants and we actually choose integer–valued invariants. Some of them were already used in [3], but here we had to define some new ones. These integer–valued invariants yield a classification which is easier to grasp.

Notation: In order to reduce the width of the upcoming tables we have renamed these invariants in the following way:

Definition 4.1 Let $I_1(S)$ denote a code given in paper [11] which describes the number and topological type of all the singularities (finite or infinite) of the phase portrait. For example $I_1(S) = 12$ means that the phase portrait has no real finite singularity and just one infinite node, or $I_1(S) = 152$ means that there is a finite saddle-node, plus an infinite node and an infinite intricate singularity which has one parabolic and one hyperbolic sector on one side of infinity, and a single flat hyperbolic sector on the other side, or even more degenerated $I_1(S) = 180$ means that the phase portrait has an infinite number of finite singularities forming an invariant straight line with no other finite singularity, plus an infinite node plus an infinite saddle-node formed by the coalescence of a finite singularity with an infinite one. In this way, two phase portraits having a different code $I_1(S)$ may never be topologically equivalent.

Definition 4.2 Let $I_2(S)$ denote a code given by the sequence of up to two digits (each one ranging from 0 to 5) such that each digit describes the total number of global or local separatrices ending (or starting) at a singular finite point. The digits are ordered in descending order.

Definition 4.3 Let $I_3(S)$ denote a code given by the sequence of digits (each one ranging from 0 to 4) such that each digit describes the total number of global or local separatrices (different from the infinity line) ending (or starting) at an infinite singular point. The number of digits in the sequences is 2, 4 or 6 depending on the number of infinite singular points. We can start the sequence at anyone of the infinite singular points but all sequences must be listed in a same specific order either clockwise or counterclockwise along the line of infinity so as to produce the biggest possible number.

Definition 4.4 Let $I_4(S)$ denote a digit that gives the number of limit cycles around a foci.

Definition 4.5 Let $I_5(S)$ denote a code which directly gives the phase portrait of systems with centers. This code is taken from the classification of quadratic systems with a center given by Vulpe in [28].

Definition 4.6 Given a finite saddle where the two stable (resp. unstable) separatrices have the same ω-limit (resp. α-limit), we will call a *basin* the set limited by those separatrices. We will say that the basin *hangs* from that ω-limit (resp. α-limit).

Definition 4.7 Let $I_6(S)$ denote a singularity (each either N or SN) such that it describes the point from which a basin hangs.

Remark 4.8 The phase portraits having neither limit cycle nor graphic have been denoted surrounded by parenthesis, for example (AV_8); the phase portraits having a limit cycle have been denoted surrounded by brackets, for example $[AV_{11}]$; the phase portraits having graphics have been denoted surrounded by {}, for example $\{A7S_3\}$. Consequently, phase portraits having a limit cycle and a graphic have been denoted surrounded by [{}], for example $[\{A5S_{11}\}]$. In some similar articles where two graphics existed we also used {{}} to denote it, but here we have examples with an infinite number of graphics (the degenerated cases), so we have preferred not to use multiple braces.

We do not distinguish between phase portraits whose only difference is that in one we have a finite node and in the other a focus. Both phase portraits are topologically equivalent and they can only be distinguished within the C^1 class. Anyway, in case we may want to distinguish between them, a new invariant may easily be introduced.

Theorem 4.9 *Consider the family IV of quadratic systems. Consider now all the phase portraits that we have obtained for this family. The values of the affine invariant* $\mathcal{I} = (I_1, I_2, I_3, I_4, I_5, I_6)$ *given in the following diagram yield a partition of these phase portraits of the family IV as follows:*

Given that we have defined 174 regions (136 in system A, 27 in system B, and 5 in each of systems C and D) and obtained only 85 portraits, it is necessary to inform the regions that are missing from the theorem. This justifies the following table for locating the missing phase portraits. We write in the same line of boxes all phase portraits which are topologically equivalent. And we group them in columns according to the main fact which produces the equivalence. For example in the second column we have phase portraits with a multiple singularity which behaves exactly the same just simple; in the third and fourth column respectively, we have phase portraits which have a weak focus or a weak saddle respectively; in the fifth column we have phase portraits which have an invariant straight line which is not a separatrix connection, and finally in the last column we have put the rest of cases with phase portraits which are already represented by others and the reason are different from the previous ones. For example, when we cross a dotted bifurcation and the regions have different name, they will have equivalent phase portraits.

$$
I_1 = \begin{cases}
12\ (AV_8) \\
23\&\ I_2 = \begin{cases} 40\ \{A7S_3\} \\ 41\&\ I_4 = \begin{cases} 0\ (AV_9) \\ 1\ [AV_{11}] \end{cases} \end{cases} \\
24\ \{B3S_5\}\ I_5 = Vul_2 \\
44\ (A2S_6) \\
47\ (A2.3L_2) \\
85\&\ I_3 = \begin{cases} 110100\ (A1.4L_2) \\ 110110\ (A1S_4) \\ 111010\ \{A1.7L_1\} \\ 111110\ (A1S_5) \\ 211010\&\ I_4 = \begin{cases} 0\ (A1S_2) \\ 1\ [A1S_6] \end{cases} \end{cases} \\
87\&\ I_3 = \begin{cases} 111010\ (A1.4L_1) \\ 2211110\ (A1S_1) \end{cases} \\
88\ \{A1.5L_1\} \\
89\ \{A1.5L_2\} \\
90\ \{AP_9\}\ I_5 = Vul_{14} \\
93\ (C1S_2) \\
94\ \{D1S_2\}\ I_5 = Vul_{13} \\
124\ (A4.5L_2) \\
132\&\ I_3 = \begin{cases} 111110\ (A4S_{10}) \\ 111111\ \{A7S_5\} \\ 210110\ (A4S_9) \\ 211110\ (AV_{13}) \\ 211111\&\ I_4 = \begin{cases} 0\ (AV_{18}) \\ 1\ [AV_{19}] \end{cases} \\ 220110\ \{A7S_4\} \\ 320110\&\ I_4 = \begin{cases} 0\ (AV_{14}) \\ 1\ [AV_{15}] \end{cases} \end{cases} \\
133\&\ I_5 = \begin{cases} Vul_{16}\ \{B3S_3\} \\ Vul_{17}\ \{A3.4L_1\} \\ Vul_{18}\ \{B3S_2\} \end{cases} \\
134\&\ I_3 = \begin{cases} 111010\ (A4S_1) \\ 111110\ (AV_1) \\ 211010\ (A7S_2) \\ 211110\ (AV_2) \\ 311010\ \{A7S_1\} \\ 321010\ (AV_3) \\ 411010\&\ I_4 = \begin{cases} 0\ (AV_5) \\ 1\ [AV_6] \end{cases} \end{cases} \\
\geq 135\text{followonthenextpages}
\end{cases}
$$

$$
I_1 = \begin{cases}
135\&\ I_3 = \begin{cases} 2100\ (A5.7L_2) \\ 2101\ (A5S_1) \\ 2200\ \{A5.7L_1\} \\ 3200\&\ I_4 = \begin{cases} 0\&\ I_6 = \begin{cases} N\ (A5S_4) \\ SN\ (A5S_6) \end{cases} \\ 1\ [A5S_5] \end{cases} \end{cases} \\
136\&\ I_2 = \begin{cases} 40\ \{A5.7L_3\} \\ 41\&\ I_3 = \begin{cases} 1110\ \{A4.5L_4\} \\ 2210\ \{A5S_{12}\} \\ 3101\&\ I_4 = \begin{cases} 0\ \{A5S_{10}\} \\ 1\ [\{A5S_{11}\}] \end{cases} \end{cases} \\ 42\ \{A5S_8\} \end{cases} \\
137\ (A4.5L_1) \\
140\ (AV_{12}) \\
141\ (AV_4) \\
142\ (A5S_2) \\
143\ \{A5S_9\} \\
144\ (AP_1) \\
148\&\ I_3 = \begin{cases} 210110\ (A2.4L_3) \\ 211110\ (A2S_8) \\ 320110\ (A2S_9) \end{cases} \\
149\&\ I_3 = \begin{cases} 111010\ (A2.4L_1) \\ 111110\ (A2S_2) \\ 211010\ (A2.7L_1) \\ 211110\ (A2S_1) \\ 321010\ (A2S_4) \\ 411010\ (A2S_5) \end{cases} \\
150\&\ I_3 = \begin{cases} 110000\ (B2.3L_1) \\ 220110\ (A2.3L_3) \end{cases} \\
151\ (A2.3L_1) \\
152\&\ I_3 = \begin{cases} 2100\ (AP_2) \\ 2101\ (A2.5L_1) \\ 3200\&\ I_6 = \begin{cases} N\ (A2.5L_3) \\ SN\ (A2.5L_4) \end{cases} \end{cases} \\
153\ (AP_3) \\
154\&\ I_3 = \begin{cases} 1101\ \{AP_4\} \\ 2101\ \{A2.5L_5\} \\ 2201\ \{A2.5L_6\} \\ 3101\ \{A2.5L_7\} \end{cases} \\
155\ \{AP_5\} \\
165\ \{C1.1L_2\} \\
180\ \{AP_6\} \\
193\ \{CP_1\} \\
195\ (DP_1)
\end{cases}
$$

Appendix A

Very recently a paper [2] has appeared with the complete study of class I of Ye [29]. This class is part of a set of three normal forms (I, II and III) which covers all possible systems having a limit cycle and have been widely studied since they were first proposed. Notice that classes I, II and III of Ye [29] have nothing to do with Families 1, II and III of (2).

Specially class I which only has 4 parameters can be written as:

$$\dot{x} = y, \qquad \dot{y} = -x + by + \ell x^2 + mxy + ny^2. \tag{12}$$

Clearly this class is a subset of family IV which guarantee the existance of an isolated antisaddle (focus, node or center) at the origin plus maybe another finite isolated singularity, while family IV may have either no real finite singularity, or a saddle-node, or a cusp, or even be a degenerate system. So all the phase portraits found in [2] are present here, and some of the phase portraits here cannot be present in [2]. Somehow, the results of [2] have been confirmed here using a more general normal form.

This can be easily checked: Since both works use the same topological invariants to detect coincidences among phase portraits inside each paper, now it is very easy to check if the invariants of the phase portraits of one paper coincide with those of the other paper. When they differ, they must be different, if they coincide, there is a high probability that they are the same, and some further check must be done to confirm this, or to find some other invariant that distinguishes them.

In this way the phase portraits of this paper named:

- AV_4, AV_8, AV_{12}, $A5S_2$, $A5S_9$, $A4.5L_1$ and $C1.1L_2$ have no correspondence in [2] because they have no finite singular points;
- $A2S_1$, $A2S_2$, $A2S_4$, $A2S_5$, $A2S_6$, $A2S_8$, $A2S_9$, $A2.4L_1$, $A2.4L_3$, $A2.5L_1$, $A2.5L_3$, $A2.5L_4$, $A2.5L_5$, $A2.5L_6$, $A2.5L_7$, $A2.7L_1$, AP_1, AP_2 and AP_4 have no correspondence in [2] because their only finite singularity is a saddle-node;
- $A2.3L_1$, $A2.3L_2$, $A2.3L_3$, AP_3, AP_5 and $B2.3L_1$ have no correspondence in [2] because their only finite singularity is a cusp;
- $A1S_1$, $A1.4L_1$ and $A1.5L_1$ have no correspondence in [2] because their only finite singularity is a saddle;
- AP_6, CP_1 and DP_1 have no correspondence in [2] because they are degenerate systems.

The phase portraits found in both papers are given in Table 2.

Remark 5.1 The similarities between the codes given in the phase portraits of both papers are not casual. Since in both papers the algorithm to assign names is the same, it is normal that the code given to phase portraits for invariant straight lines (4 S) appears on both cases (like others) and that generic phase portraits in one family, be also generic in the other.

The order given in Table 2 s due to the topological invariants used which is the simplest way to compare both lists in an Excel file.

Table 2 Coincidences with [2]

Phase portrait	In [2]	I_1	I_2	I_3	Other invariant
$A7S_3$	$7S_1$	23	40	11	
AV_9	V_1	23	41	21	$I_4 = 0$
AV_{11}	V_5	23	41	21	$I_4 = 1$
$B3S_5$	$3.8L_1$	24			$I_5 = Vul_2$
$A1.7L_1$	$1.7L_1$	85	0	111010	
$A1.4L_2$	$1.4L_2$	85	1	110100	
$A1S_5$	$1S_4$	85	1	111110	
$A1S_2$	$1S_6$	85	1	211010	$I_4 = 0$
$A1S_6$	$1S_5$	85	1	211010	$I_4 = 1$
$A1S_4$	$1S_1$	85	2	110110	
$A1.5L_2$	$1.9L_1$	89	1	1110	
AP_9	P_{11}	90			$I_5 = Vul_{14}$
$C1S_2$	$1.8L_1$	93	1	2100	
$D1S_2$	P_9	94			$I_5 = Vul_{13}$
$A4.5L_2$	$4.5L_1$	124	43	2120	
$A7S_5$	$7S_4$	132	40	111111	
$A7S_4$	$7S_5$	132	40	220110	
$A4S_{10}$	$4S_5$	132	41	111110	
$A4S_9$	$4S_6$	132	41	210110	
AV_{18}	V_{14}	132	41	211111	$I_4 = 0$
AV_{19}	V_{13}	132	41	211111	$I_4 = 1$
AV_{14}	V_{29}	132	41	320110	$I_4 = 0$
AV_{15}	V_{31}	132	41	320110	$I_4 = 1$
AV_{13}	V_{15}	132	42	211110	
$B3S_3$	$3.8L_2$	133			$I_5 = Vul_{16}$
$A3.4L_1$	$4.7L_1$	133			$I_5 = Vul_{17}$
$B3S_2$	$3.8L_3$	133			$I_5 = Vul_{18}$
$A7S_1$	$7S_2$	134	40	311010	
$A7S_2$	$7S_3$	134	41	211010	
AV_3	V_8	134	41	321010	
AV_5	V_2	134	41	411010	$I_4 = 0$
AV_6	V_6	134	41	411010	$I_4 = 1$
$A4S_1$	$4S_1$	134	42	111010	
AV_2	V_9	134	42	211110	
AV_1	V_{12}	134	43	111110	
$A5.7L_1$	$5.7L_1$	135	40	2200	
$A5.7L_2$	$5.7L_2$	135	41	2100	
$A5S_4$	$5S_6$	135	41	3200	$(I_4, I_6) = (0, N)$
$A5S_6$	$5S_4$	135	41	3200	$(I_4, I_6) = (0, SN)$
$A5S_5$	$5S_5$	135	41	3200	$I_4 = 1$
$A5S_1$	$5S_1$	135	42	2101	

Table 2 continued

Phase portrait	In [2]	I_1	I_2	I_3	Other invariant
$A5.7L_3$	$7.9L_1$	136	40	2101	
$A4.5L_4$	$4.9L_1$	136	41	1110	
$A5S_{12}$	$9S_4$	136	41	2210	
$A5S_{10}$	$9S_1$	136	41	3301	$I_4 = 0$
$A5S_{11}$	$9S_3$	136	41	3301	$I_4 = 1$
$A5S_8$	$9S_6$	136	42	2101	

Remark 5.2 Even though one of the authors is common in both papers, the history behind each paper is quite different. Paper [2] was initiated several years ago by Hebai and Jia while this paper was initiated some months ago by Cairo and Llibre in an independent way, both trying it with classical techniques. So, when the rest of authors joined the respective teams and the works could be completed with the newer tools, we realized that [2] was going to be overcome by this paper but we considered more correct to complete them in the order in which they were initiated and give credit to all the authors.

Acknowledgements The first and third authors are partially supported by the Agencia Estatal de Investigación of Spain grants PID2022-136613NB-100 and the Agència de Gestió d'Ajuts Universitaris i de Recerca grant 2021SGR00113. J. Llibre is also partially supported by the Real Academia de Ciències i Arts de Barcelona. We also want to thank the referees for their good job.

Author Contributions Cairo and Llibre have already studied the less generic families of (2), using classical techniques. And they tried to do the same with family IV. But family IV was too generic to be studied with such techniques, and Artés was added so to introduce the new more powerful techniques based on invariants which have helped to complete the classification.

Funding Open Access Funding provided by Universitat Autonoma de Barcelona.

Data Availibility Statement No datasets were generated or analysed during the current study.

Declarations

Conflict of interest The authors declare no competing interests.

References

1. Álvarez, M.J., Ferragud, A., Jarque, X.: A survey on the blow up technique. Int. J. Bifur. Chaos **21**, 3103–3118 (2011)

2. Artés, J.C., Chen, H., Ferrer, L.M., Jia, M.: Quadratic vector fields in class I, Dyn. Syst. (2024). https://doi.org/10.1080/14689367.2024.2436223
3. Artés, J.C., Llibre, J., Schlomiuk, D.: The geometry of quadratic differential systems with a weak focus of second order. Int. J. Bifur. Chaos Appl. Sci. Eng. **16**, 3127–3194 (2006)
4. Artés, J.C., Llibre, J., Schlomiuk, D.: The geometry of quadratic polynomial differential systems with a weak focus and an invariant straight line. Int. J. Bifur. Chaos Appl. Sci. Eng. **20**(11), 3627–3662 (2010)
5. Artés, J.C., Llibre, J., Schlomiuk, D., Vulpe, N.: Invariant conditions for phase portraits of quadratic systems with complex conjugate invariant lines meeting at a finite point. Rend. Circ. Mat. Palermo **70**(2), 923–945 (2021)
6. Artés, J.C., Mota, M.C., Rezende, A.C.: Quadratic differential systems with a finite saddle-node and an infinite saddle-node (1, 1)SN - (A). Int. J. Bifur. Chaos Appl. Sci. Eng. **31**(2), 2150026 (2021)
7. Artés, J.C., Mota, M.C., Rezende, A.C.: Quadratic differential systems with a finite saddle-node and an infinite saddle-node (1, 1)SN - (B). Int. J. Bifur. Chaos Appl. Sci. Eng. **31**(9), 2021c2130026 (2021)
8. Artés, J.C., Rezende, A.C., Oliveira, R.: Global phase portraits of quadratic polynomial differential systems with a semi-elemental triple node. Int. J. Bifur. Chaos Appl. Sci. Eng. **23**(8), 1350140 (2013)
9. Artés, J.C., Rezende, A.C., Oliveira, R.: The geometry of quadratic polynomial differential systems with a finite and an infinite saddle-node (A, B). Int. J. Bifur. Chaos Appl. Sci. Eng. **24**(4), 1450044 (2014)
10. Artés, J.C., Rezende, A.C., Oliveira, R.D.S.: The geometry of quadratic polynomial differential systems with a finite and an infinite saddle-node (C). Int. J. Bifur. Chaos Appl. Sci. Eng. **25**(3), 1530009 (2015)
11. Artés, J.C., Llibre, J., Schlomiuk, D., Vulpe, N.: Global topological configurations of singularities for the whole family of quadratic differential systems. Qual. Theory Dyn. Syst. **19**(51), 1–32 (2020)
12. Artés, J.C., Llibre, J., Schlomiuk, D., Vulpe, N.: Geometric Configurations of Singularities of Planar Polynomial Differential Systems. A Global Classification in the Quadratic Case, Birkhäuser (2021)
13. Büchel, W.: Zur topologie der durch eine gewöhnliche differentialgleichung erster ordnung und ersten grades definierten kurvenschar. Mitteil. der Math. Gesellsch. in Hamburg **4**, 33–68 (1904)
14. Bujac, C., Schlomiuk, D., Vulpe, N.: The bifurcation diagram of the configurations of invariant lines of total multiplicity exactly three in quadratic vector fields. Bul. Acad. tiine Repub. Mold. Mat. **1**, 42–77 (2023)
15. Cairó, L., Llibre, J.: Phase portraits of families VII and VIII of the quadratic systems. Axioms (2023). https://doi.org/10.3390/axioms12080756
16. Chicone, C., Tian, J.: On general properties of quadratic systems. Am. Math. Mon. **89**(3), 167–178 (1982)
17. Coppel, W.A.: A survey of quadratic systems. J. Differ. Equ. **2**, 293–304 (1966)
18. Dumortier, F., Llibre, J., Artés, J.C.: Qualitative Theory of Planar Differential Systems. Universitext, Springer (2006)
19. Gasull, A., Li-Ren, S., Llibre, J.: Chordal quadratic systems. Rocky Mountain J. Math. **16**, 751–782 (1986)
20. Reyn, J.: Phase Portraits of Planar Quadratic Systems, Mathematics and Its Applications vol. **583**, Springer (2007)
21. Rychkov, G.S.: A complete investigation of the number of limit cycles of the equation $(b_{10}x + y)dy = \sum_{i+j=1}^{2} a_{ij}x^i y^j dx$. Differ. Equa. **6**, 2193–2199 (1970). (**(in Russian)**)
22. Schlomiuk, D., Vulpe, N.: Planar quadratic differential systems with invariant straight lines of at least five total multiplicity. Qual. Theory Dyn. Syst. **5**(1), 135–194 (2004)
23. Schlomiuk, D., Vulpe, N.: Integrals and phase portraits of planar quadratic differential systems with invariant lines of at least five total multiplicity. Rocky Mountain J. Math. **38**(6), 2015–2075 (2008)
24. Schlomiuk, D., Vulpe, N.: Integrals and phase portraits of planar quadratic differential systems with invariant lines of total multiplicity four. Bul. Acad. Ştiinţe Repub. Mold. Mat. **1**(56), 27–83 (2008)
25. Schlomiuk, D., Vulpe, N.: Planar quadratic differential systems with invariant straight lines of total multiplicity four. Nonlinear Anal. **68**(4), 681–715 (2008)
26. Schlomiuk, D., Vulpe, N.: Global classification of the planar Lotka-Volterra differential systems according to their configurations of invariant straight lines. J. Fixed Point Theory Appl. **8**(1), 177–245 (2010)
27. Schlomiuk, D., Vulpe, N.: Global topological classification of Lotka-Volterra quadratic differential systems. Electron. J. Differ. Equ. **2012**(64), 69 (2012)
28. Vulpe, N.I.: Affine-invariant conditions for the topological discrimination of quadratic systems with a center. Differ. Equ. **19**, 273–280 (1983)

29. Ye, Y.: Theory of imit cycles, Transl. Math. Monogr., vol. **66**, Amer. Math. Soc., Providence, RI (1986)